Structural Eng. / Earthquake Eng. Vol. 7. No. 2, 313s-322s. October 1990
Japan Society of Civil Engineers (Proc. of JSCE No. 422/I-14)

EFFECT OF SPATIAL RANDOMNESS OF RESPONSE CHARACTERISTICS ON SEISMIC STABILITY OF EARTH DAMS

By Kazuta HIRATA and Masanobu SHINOZUKA***

A practical method for the stochastic analysis of the effect of spatial randomness of earth dams on the seismic stability is proposed, where attention is paid particularly to the shear strain in the horizontal cross-section due to relative displacement of the dam along its longitudinal axis. The method takes into consideration both spatial variabilities in the dam material and geometry and randomness of the earthquake motion. The proposed method is used to determine the depth-wise distribution of shear stress in the horizontal cross-section of the dam as well as that in the transverse cross-section. Such a distribution of a shear stress is in turn used to examine their effect on the seismic stability of the dam.
Keywords : earth dam, seismic stability, spatial randomness

1. INTRODUCTION

The stability analysis of earth dams during earthquake is usually performed utilizing a two-dimensional model consisting of representative transverse cross-section under plane strain condition. However, when the cross-section is not uniform as in the case where the dam is constructed in a narrow canyon and bounded by sloping canyon walls, the effect of the three-dimensional shape of the dam can be significant. The three-dimensional effect of the earth dam has been investigated by comparing the result of two-dimensional analysis with that of three-dimensional one, and its effect on the response characteristics is indicated to be significant in the case where the dam is bounded by sloping canyon walls[1)~3)].

On the other hand, regarding the seismic design of buried pipeline structures, method of stochastic estimation of ground deformation during earthquake is proposed by Harada and Shinozuka[4),5)], where the horizontal ground is modeled with the assembly of shear column and the two-dimensional effect of the ground is taken into account by introducing the correlation of response characteristics of each shear column represented as one-dimensional homogeneous random field, and the spatial distribution of relative displacement of the ground is estimated.

In this paper, a method of estimating the effect of spatial randomness of response characteristics of the earth dam on its seismic stability is presented where above mentioned method for the estimation of the relative displacement of the ground is expanded for inhomogeneous random field. The results are given in terms of the (a) variance of the relative displacement, (b) expected maximum value of the strain and (c) expected value of local safety factor during earthquake.

* Member of JSCE, M. Eng., Central Res. Inst. of Electric Power Industry (Abiko-shi, Chiba, JAPAN)
** Prof. Dep. of Civil Eng. and Operations Res. Princeton Univ. (Princeton, NJ, USA)

2. EQUATION OF MOTION

Consider an earth dam constructed in a triangular canyon as shown in Fig. 1. Input earthquake motion is considered to be vertically incident SH wave with its amplitude in the upstream-downstream direction. The arrival time of the wave at the base varies according to its elevation. Here the dam is modeled as an assembly of shear wedges as also shown in Fig. 1. From the equilibrium of shear element in the wedge, the equation of motion is given as follows[6].

$$\rho B(y,z)(\partial^2/\partial t^2)[u_b(y,t)+u_r(y,z,t)]=(\partial/\partial z)[B(y,z)\tau_{xz}] \quad (1)$$

where ρ is the mass density, B is half the width of the wedge, τ_{xz} is the shear stress in the x-z plane of the wedge, and u_b is the displacement at the base of the wedge and u_r is the relative displacement to the base. Relative displacement u_r of the wedge is expressed as a sum of the modal shape function multiplied by normal coordinate x_i as follows.

$$u_r(y,z,t)=\sum_{i=1}^{\infty} J_0(\lambda_i z/L(y))x_i(t) \quad (2)$$

where J_0 is Bessel function of the first kind of order 0, λ_i is the i-th root satisfying $J_0(\lambda)=0$ and $L(y)$ is the height of the dam in the transverse cross section at y. The normal coordinate x_i is given as a solution of the equation below.

$$\ddot{x}_i(t)+2h_i\omega_i\dot{x}(t)+\omega_i^2 x_i(t)=-\beta_i\ddot{u}_b(t) \quad (i=1,2\cdots) \quad (3)$$

where $\cdot$ means time derivative, h_i and ω_i are modal damping ratio and natural angular frequency for i-th mode, and ω_i is given from the equation below

$$\omega_i L/C_{SD}=\lambda_i \quad (i=1,2\cdots) \quad (4)$$

where C_{SD} is the shear wave velocity of the dam and β_i is the modal participation factor expressed as

$$\beta_i=\int_0^L zJ_0(\lambda_i z/L)dz \Big/ \int_0^L z[J_0(\lambda_i z/L)]^2 dz \quad (5)$$

3. SPATIAL VARIABILITY OF RESPONSE

(1) Spatial distribution of natural frequency and damping

Response characteristics of the shear wedge represented by the resonance frequency and modal damping ratio are dependent on the wedge location specified by y. The spatial variability of resonance angular frequency $\omega_i^*(y)$ and the modal damping ratio $h_i^*(y)$ are expressed as follows[4),5)].

$$\omega_i^*(y)=\omega_i(y)[1+f(y)], \quad h_i^*(y)=h_i(y)[1+h(y)] \quad (6)$$

where $\omega_i(y)$ and $h_i(y)$ are the mean values of $\omega_i^*(y)$ and $h_i^*(y)$, and $f(y)$ and $h(y)$ are homogeneous stochastic fields which are considered resulting from the randomness of material properties and geometry. It should be noted that although $f(y)$ and $h(y)$ are homogeneous stochastic fields, $\omega_i^*(y)$ and $h_i^*(y)$ are non-homogeneous because the mean values $\omega_i(y)$ and $h_i(y)$ are dependent on y. In Eq. (6), it is assumed that

$$E[f^2(y)]\ll 1, \quad E[h^2(y)]\ll 1 \quad (7)$$

where $E[\cdot]$ means expectation operator. Relationships between the coefficient of variation $\delta\omega_i^*$ of $\omega_i^*(y)$

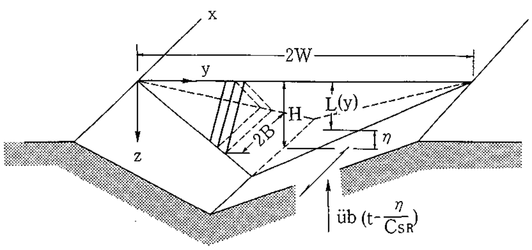

Fig. 1 Three-dimensional View of Earth Dam in Triangular Canyon and Modeling of the Dam.

and the standard deviation σ_{ff} of $f(y)$, and between the coefficient of variation δ_h^* of $h_t^*(y)$ and the standard deviation σ_{nn} of $h(y)$ are

$$\delta\omega^* = \sigma_{ff}, \quad \delta_h^* = \sigma_{hh} \qquad (8)$$

(2) Time-space correlation of displacement

In the estimation of seismic stability of earth structures such as fill dams, effect of the first mode is predominant as indicated from amplification function of the dam obtained from 3-D FEM analysis[1),3)], hence the first mode is considered and the subscript 1 in ω and h is omitted hereafter. Input acceleration motion at the base of the dam considering phase lag is given as

$$\ddot{u}_b = \ddot{u}_b(t - \eta(y)/C_{SR}) \qquad (9)$$

where $\eta(y)$ is the elevation of the base of the wedge measured from the lowest elevation of the bottom of the dam as shown in **Fig. 1**, and C_{SR} is the shear wave velocity of the foundation. Taking the first term of Eq. (2), relative displacement u_r of the dam to the ground considering spatial variability is obtained as follows.

$$u_r^*(y, z, t) = -\beta J_0(\lambda_1 z/L(y)) \int_0^\infty I^*(y, \tau)\, \ddot{u}_b(t - \tau - \eta(y)/C_{SR})\, d\tau \qquad (10)$$

where $I^*(y, \tau)$ is the impulse response function considering spatial variability, and expressed as

$$\left.\begin{aligned} I^*(\tau) &= (1/\omega^* \sqrt{1-h^{*2}}) \exp(-h^*\omega^*\tau) \sin(\omega^* \sqrt{1-h^{*2}}\, \tau) && \text{for } \tau > 0 \\ &= 0 && \text{for } \tau \leqq 0 \end{aligned}\right\} \qquad (11)$$

The total displacement of the dam is given as

$$u(y, z, t) = u_r^*(y, z, t) + u_b(t - \eta(y)/C_{SR}) \qquad (12)$$

Time-space correlation function of $u(y, z, t)$ denoted by Q_{uu} is defined by

$$Q_{uu}(y, z, t, \xi, \tau) = E[u(y, z, t)\, u(y+\xi, z, t+\tau)] \qquad (13)$$

where ξ and τ are spatial and time separations. Assuming the stationarity of u with respect to time, Q_{uu} is independent of time. Temporally spectral and spatially correlational function P_{uu} of u is defined as

$$P_{uu}(y, z, \xi, \omega) = (1/2\pi) \int_{-\infty}^{\infty} \exp(-i\omega\tau)\, Q_{uu}(y, z, \xi, \tau)\, d\tau \qquad (14)$$

and inversely

$$Q_{uu}(y, z, \xi, \tau) = \int_{-\infty}^{\infty} \exp(i\omega\tau)\, P_{uu}(y, z, \xi, \omega)\, d\omega \qquad (15)$$

Spatial correlation function R_{uu} of u is defined as

$$R_{uu}(y, z, \xi) = Q_{uu}(y, z, \xi, 0) = \int_{-\infty}^{\infty} P_{uu}(y, z, \xi, \omega)\, d\omega \qquad (16)$$

Stochastic estimation of the relative displacement of the horizontal ground during earthquake is proposed by Harada and Shinozuka[4),5)], here the method is applied to the case of the earth dam where the height varies at each transverse cross-section. As shown in Eq. (11) impulse response function includes nonlinear term with respect to ω^* and h^*, and to make linear operation possible, the impulse response function is expanded into Taylor series with respect to ω^* and h^* around their mean values ω_0 and h_0. And truncating higher terms beyond the second on the assumption that the variations of ω^* and h^* around ω_0 and h_0 are small as shown in Eq. (7), the total displacement in Eq. (12) is expressed as follows.

$$\begin{aligned} u(y, z, t) = &-\beta J_0(\lambda_1 z/L(y)) \int_0^\infty I(\omega_0(y), h_0(y), \tau)\, \ddot{u}_b(t - \tau - \eta(y)/C_{SR})\, d\tau \\ &-[\beta J_0(\lambda_1 z/L(y))\, \omega_0(y) \int_0^\infty I'_{\omega^*}(\omega_0(y), h_0(y), \tau)\, \ddot{u}_b(t - \tau - \eta(y)/C_{SR})\, d\tau] f(y) \\ &-[\beta J_0(\lambda_1 z/L(y))\, h_0(y) \int_0^\infty I'_{h^*}(\omega_0(y), h_0(y), \tau)\, \ddot{u}_b(t - \tau - \eta(y)/C_{SR})\, d\tau] h(y) \\ &+ u_b(t - \eta(y)/C_{SR}) \end{aligned} \qquad (17)$$

where I'_{ω^*} and I'_{h^*} are derivatives with respect to ω^* and h^*. Substituting Eq. (17) into Eq. (13) and further into Eq. (14) and assuming independence between $f(y)$ and $h(y)$, and neglecting terms of the second order with respect to $f(y)$ and $h(y)$, P_{uu} is given as

$$P_{uu}(y, z, \xi, \omega)=S_{\ddot{u}_b\ddot{u}_b}(\omega)\exp(-i\omega/C_{SR}[\eta(y+\xi)-\eta(y)])$$
$$\times[1/\omega^2+\beta J_0(\lambda_1 z/L(y))H(-\omega, y)][1/\omega^2+\beta J_0(\lambda_1 z/L(y+\xi)H(-\omega, y+\xi)]$$
$$+4\beta^2 R_{ff}(\xi)J_0(\lambda_1 z/L(y))J_0(\lambda_1 z/L(y+\xi)H^2(-\omega, y)H^2(\omega, y+\xi)$$
$$\times\omega_0^2(y)\omega_0^2(y+\xi)S_{\ddot{u}_b\ddot{u}_b}(\omega)\exp(-i\omega/C_{SR}[\eta(y+\xi)-\eta(y)])$$
$$\times[1+i\omega\{h_0(y+\xi)/\omega_0(y+\xi)-h_0(y)/\omega_0(y)\}] \quad (18)$$

where $S_{\ddot{u}_b\ddot{u}_b}(\omega)$ is the power spectral density of input ground acceleration and $H(\omega, y)$ is the first modal frequency response function for relative displacement given as

$$H(\omega, y)=-1/(\omega_0^2-\omega^2+i2h_0(y)\omega_0(y)\omega) \quad (19)$$

and $R_{ff}(\xi)$ is the correlation function of $f(y)$. In the derivation of Eq. (18), correlation function $R_{hh}(\xi)$ and the mean $h_0(y)$ of h are assumed to be small and terms of the second order with respect to these quantities are neglected.

4. ESTIMATION OF SHEAR STRAIN

(1) Shear strain in horizontal cross-section

Shear strain of the dam in the horizontal cross-section along the longitudinal axis can be estimated from the relative displacement of adjacent wedges as shown in **Fig. 2**. First, consider relative displacement u_D along the longitudinal (y) axis between two points specified by y and $y+D$ at a depth z from the crest.

$$u_D(y, z, D, t)=u(y+D, z, t)-u(y, z, t) \quad (20)$$

Then time-space correlation function $Q_{u_Du_D}$ of u_D is given by

$$Q_{u_Du_D}(y, z, D, \xi, \tau)=E[u_D(y, z, D, t)u_D(y+\xi, z, D, t+\tau)] \quad (21)$$

Substituting Eq. (20) into Eq. (21), and using the relationship shown in Eq. (13), then substituting $\tau=0$, the spatial correlation function $R_{u_Du_D}$ of u_D is derived as

$$R_{u_Du_D}(y, z, D, \xi)=Q_{u_Du_D}(y, z, D, \xi, 0)$$
$$=R_{uu}(y+D, z, \xi)+R_{uu}(y, z, \xi)-R_{uu}(y, z, D+\xi)$$
$$-R_{uu}(y+D, z, \xi, -D) \quad (22)$$

Variance $\sigma_{u_Du_D}^2$ of u_D is given using Eq. (16) as

$$\sigma_{u_Du_D}^2=R_{u_Du_D}(y, z, D, 0)$$
$$=\int_{-\infty}^{\infty}P_{uu}(y+D, z, 0, \omega)d\omega+\int_{-\infty}^{\infty}P_{uu}(y, z, 0, \omega)d\omega-2\int_{-\infty}^{\infty}P_{uu}(y, z, D, \omega)d\omega \quad (23)$$

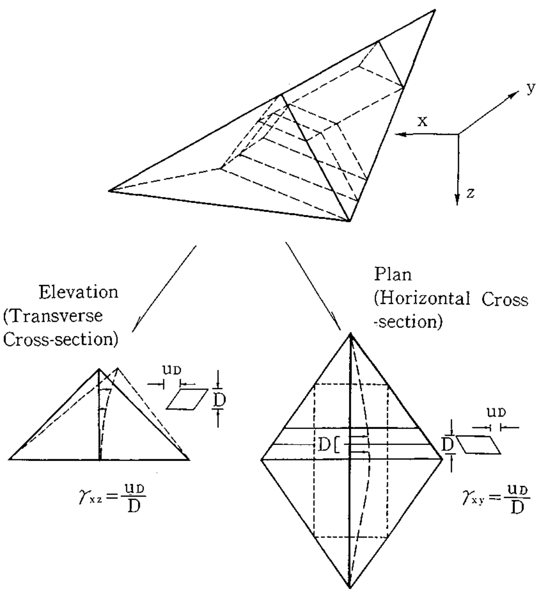

Fig. 2 Definition of Shear Strain γ_{xz} and γ_{xy}.

As for the shear strain, consider the local average γ_D of shear strain γ_{xy} defined by

$$\gamma_D(y)=(1/D)\int_y^{y+D}\gamma_{xy}(y)dy=(1/D)u_D(y) \qquad (24)$$

And the variance $\sigma^2_{\gamma_D\gamma_D}$ of $\gamma_D(y)$ is given by Eqs. (23) and (24)

$$\sigma^2_{\gamma_D\gamma_D}=(1/D^2)\sigma^2_{uDuD} \qquad (25)$$

After the variance of shear strain is obtained, one can estimate expected maximum value of shear strain using peak factor, PFA, derived from probability distribution for extreme values as follows[7),8)]

$$(\gamma_D)_{\max}=PFA\cdot\sigma_{\gamma_D\gamma_D}$$
$$PFA\fallingdotseq\sqrt{2\ln(2\nu T)}+\gamma/\sqrt{2\ln(2\nu T)} \qquad (26)$$

where ν is the apparent frequency of the process, T is the duration of the process and γ is the Euler's constant (=0.5772…). The apparent frequency ν of the process is defined as

$$\nu=(1/2\pi)(m_2/m_0)^{1/2} \qquad (27)$$

where m_0 and m_2 are spectral moment of order of zero and 2 and defined as

$$m_0=\int_{-\infty}^{\infty}S(\omega)d\omega,\quad m_2=\int_{-\infty}^{\infty}\omega^2S(\omega)d\omega \qquad (28)$$

with $S(\omega)$ being the power spectral density of the process.

(2) Shear strain in transverse cross-section

Shear strain in the transverse cross-section can be estimated from the relative displacement along the vertical axis in the shear wedge at each section in the similar way to the case of horizontal cross-section. However, as to the shear strain γ_{xz} in the transverse cross-section, the relationship between displacement and shear strain can be made use of given as

$$\gamma_{xz}=\partial u(y,z,t)/\partial z \qquad (29)$$

Substituting Eq. (17) into Eq. (29) one can obtain

$$\gamma_{xz}(y,z,t)=(\beta\lambda_1/L(y))J_0(\lambda_1z/L(y))$$
$$\Big[\int_0^\infty I(\omega_0(y),h_0(y),\tau)u_b(t-\tau-\eta(y)/C_{SR})d\tau$$
$$+\omega_0(y)f(y)\int_0^\infty I'_{\omega^*}(\omega_0(y),h_0(y),\tau)u_b(t-\tau-\eta(y)/C_{SR})d\tau$$
$$+h_0(y)h(y)\int_0^\infty I'_{h^*}(\omega_0(y),h_0(y),\tau)u_b(t-\tau-\eta(y)/C_{SR})d\tau\Big] \qquad (30)$$

where the relationship below is used.

$$\partial/\partial z[J_0(\lambda_1z/L(y))]=-[\lambda_1/L(y)]J_1(\lambda_1z/L(y)) \qquad (31)$$

where J_1 is the Bessel function of the first kind of order 1.

The variance of the shear strain γ_{xz} is obtained as

$$\sigma^2_{\gamma_{xz}\gamma_{xz}}=\int_0^\infty P_{\gamma_{xz}\gamma_{xz}}(y,z,\omega)d\omega \qquad (32)$$

where $P_{\gamma_{xz}\gamma_{xz}}$ is the power spectral density function of γ_{xz} which is given as

$$P_{\gamma_{xz}\gamma_{xz}}(y,z,\omega)$$
$$=S_{\ddot u_b\ddot u_b}(\omega)[\{(\beta\lambda_1/L(y))J_0(\lambda_1z/L(y))\}^2|H(\omega,y)|^2$$
$$-(2\beta\lambda_1/\omega^2L(y))J_1(\lambda_1z/L(y))(\omega_0^2(y)-\omega^2)|H(\omega,y)|^2]$$
$$+4\beta^2R_{ff}(0)\omega_0^4(y)S_{\ddot u_b\ddot u_b}(\omega)\{(\lambda_1/L(y))J_1(\lambda_1z/L(y))\}^2|H(\omega,y)|^4 \qquad (33)$$

5. INPUT EARTHQUAKE MOTION

As the power spectrum $S_{\ddot u_b\ddot u_b}(\omega)$ of input acceleration motion, the filtered Kanai-Tajimi spectrum[9)] given below is used in which singularity at $\omega=0$ is removed to make the estimation of displacement variance possible.

$$S_{\ddot u_b\ddot u_b}(\omega)=S_A(\omega)(\omega/\omega_f)^4/[\{1-(\omega/\omega_f)^2\}^2+4\zeta_f^2(\omega/\omega_f)^2] \qquad (34)$$

with $S_A(\omega)$ being the Kanai-Tajimi spectrum[10),11)] given as

$$S_A(\omega)=S_0[1+4\zeta_g^2(\omega/\omega_g)^2]/[\{1-(\omega/\omega_g)^2\}^2+\{2\zeta_g(\omega/\omega_g)\}^2] \qquad (35)$$

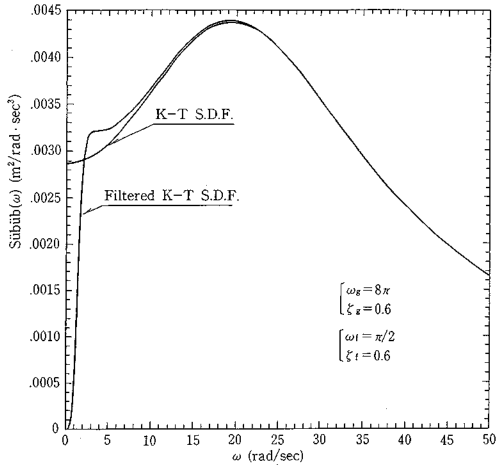

Fig. 3 Power Spectral Density of Input Acceleration (Filtered and Non-filtered Kanai-Tajimi Spectrum).

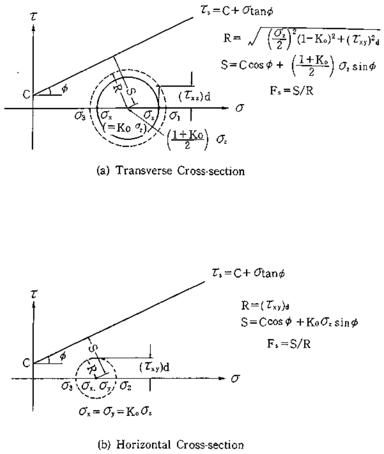

Fig. 4 Definition of Local Safety Factor.

where S_0 is the intensity of white noise, ζ_g and ω_g are damping ratio and natural frequency when the ground is considered as a SDOF system, and ζ_f and ω_f are damping and frequency parameters determined to give desired filter characteristics.

Fig. 3 shows both filtered and unfiltered Kanai-Tajimi spectrum. The former one is used in the numerical calculations afterwards. Parameters used are $\omega_g=8\pi$ (rad/sec), $\zeta_g=0.6$, which are so selected to represent earthquake accelerograms observed on the bedrock or stiff soil[12], and ω_f and ζ_f are given as $\omega_f=\pi/2$ (rad/sec), $\zeta_f=0.6$.

6. ESTIMATION OF LOCAL SAFETY FACTOR

The local safety factor is defined as the ratio of the available shear strength to the shear stress acting at each portion of the dam as shown in Fig. 4. Spatial distribution of the local safety factor gives the information as to the occurrence of the local fracture in the dam, and is made use of in the assumption of the potential sliding surface. Before earthquake, static σ_x, σ_y and σ_x, σ_z are acting in the $x-y$ and $x-z$ plane, and from the assumption of isotropic stress condition, $\sigma_x=\sigma_y$ (i.e., $\tau_{xy}=0$). During earthquake, additional dynamic shear stresses $(\tau_{xy})_d$ and $(\tau_{xz})_d$ are generated in each section. The local safety factors $(F_s)_{xy}$ and $(F_s)_{xz}$ in the $x-y$ plane (horizontal cross-section) and $x-z$ plane (transverse cross-section) are defined as the ratio of the distance from the center of Mohr's stress circle to the fracture surface to the radius of Mohr's circle[13], and given as

$$(F_s)_{xy}=(C\cos\phi+K_0\sigma_z\sin\phi)/(\tau_{xy})_d$$
$$(F_s)_{xz}=(C\cos\phi+\{(1+K_0)/2\}\sigma_z\sin\phi]/[(\sigma_z/2)^2(1-K_0)^2+(\tau_{xz})_d^2]^{1/2} \quad \cdots\cdots (36)$$

where σ_z is the normal stress in z-direction and other normal stress components σ_x and σ_y are evaluated using coefficient of lateral stress at rest K_0 defined as the ratio of horizontal normal stress to that of vertical normal stress, and Mohr-Coulomb's failure criterion for the dam material given below is made use of.

$$\tau_s=C+\sigma\tan\phi \quad \cdots\cdots (37)$$

where τ_s is the shear strength, C is the cohesion, σ is the normal stress on the shear surface and ϕ is the friction angle.

7. NUMERICAL RESULTS

(1) Spatial distribution of shear strain

According to the method presented in the previous chapters stochastic estimation of the earth dam during

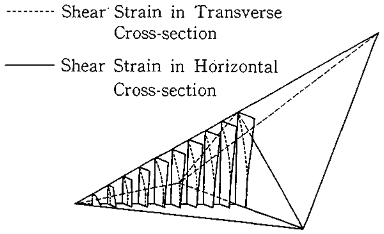

Fig. 5 Schematic View of Spatial Distribution of Shear Strain in Horizontal and Transverse Cross-sections.

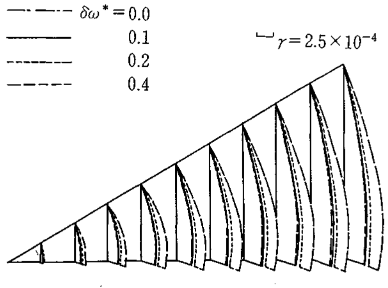

Fig. 8 Spatial Distribution of Expected Maximum Shear Strain in Transverse Cross-section (Parameter : c. o. v. of Natural Frequency, b=10 m).

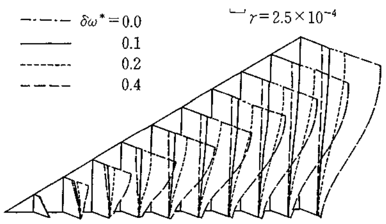

Fig. 6 Spatial Distribution of Expected Maximum Shear Strain in Horizontal Cross-section (Parameter : c. o. v. of Natural Frequency, b=10 m).

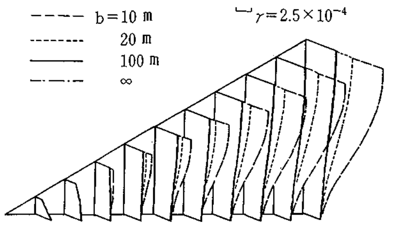

Fig. 7 Spatial Distribution of Expected Maximum Shear Strain in Horizontal Cross-section (Parameter : Correlation Distance b, $\delta\omega^*$=0. 1).

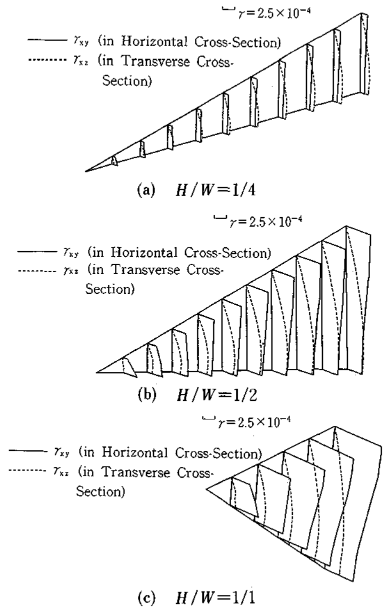

Fig. 9 Effect of Canyon Slope H/W on Spatial Distribution of Expected Maximum Shear Strain (b=10 m, $\delta\omega^*$=0. 1).

earthquake is made. The variance of the shear strain is evaluated by the numerical integration of the power spectral density given by Eq. (23) and (33). Spatial correlation function $R_{ff}(\xi)$ of $h(y)$ is assumed as a function of negative exponential one as

$$R_{ff}(\xi)=\sigma_{ff}^2\exp(-(\xi/b)^2) \qquad (38)$$

Schematic view of the spatial distribution of the shear strain due to earthquake is shown in Fig. 5 where the spatial distributions of the shear strain both in the transverse cross-section and horizontal cross-section are shown with dotted line and solid line respectively.

Figs. 6 and 7 show the spatial distribution of the expected maximum shear strain $(\gamma_{xy})_{\max}$ in the horizontal cross-section with c. o. v. $\delta\omega^*$ $(=\sigma_{ff}$ from Eq. (8)) and correlation distance b of natural angular frequency of the shear wedges being parameters. As for the effect of $\delta\omega^*$ shown in Fig. 6, the shear strain γ_{xy} increases as $\delta\omega^*$ increases indicating that as the randomness with respect to the response characteristics of shear wedge increases the relative displacement between the wedges increases. As for the effect of correlation distance b shown in Fig. 7, the shear strain $(\gamma_{xy})_{\max}$ decreases as b increases, and in the case $b=\infty$, i. e., under the condition of full coherence of $f(y)$, the strain becomes smallest, which gives the lower bound of the expected maximum shear strain. In these cases the shear strain increases as

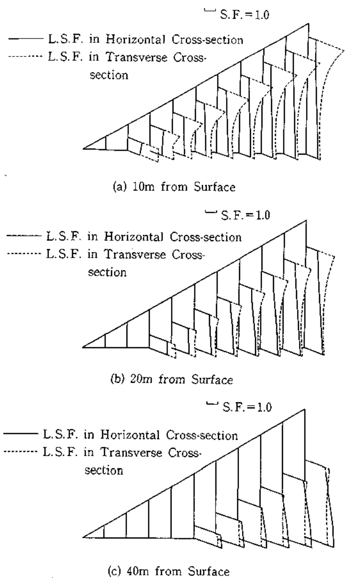

Fig. 10 Spatial Distribution of Expected Minimum Local Safety Factor (Canyon Slope $H/W=1/2$, $b=10$ m, $\delta\omega^*=0.1$).

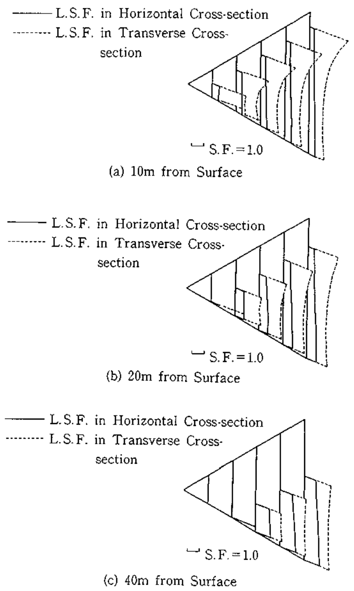

Fig. 11 Spatial Distribution of Expected Minimum Local Safety Factor (Canyon Slope $H/W=1/1$, $b=10$ m, $\delta\omega^*=0.1$).

the level becomes higher and as the height of the crest from the base increases. The former trend is wholly contrary to the spatial distribution pattern of the shear strain in the transverse cross-section as will be shown afterwards.

Fig. 8 shows the spatial distribution of the expected maximum shear strain $(\gamma_{xz})_{\max}$ in the transverse cross-section with c. o. v. of natural frequency of the shear wedges as a parameter. In this case shear strain becomes zero at the crest level from the boundary condition of zero stress there, and shear strain increases as the level decreases. This trend of the shear strain distribution can usually be observed in the two-dimensional response analysis, where the shear strain distribution in the horizontal cross-section cannot be taken into account. The effect of the parameter, c. o. v. of the natural frequency, is not so conspicuous as that for the strain in the horizontal cross-section. Fig. 9 shows the spatial distribution of the expected maximum shear strain both in the horizontal and transverse cross-sections with different canyon slope. As the canyon slope becomes steeper, $(\gamma_{xy})_{\max}$ in the horizontal cross-section increases, whereas $(\gamma_{xz})_{\max}$ in the transverse cross-section is not affected by the canyon slope.

(2) Spatial distribution of local safety factor

In the estimation of the local safety factor, K_0 of 0.5, cohesion C of 10.0 (tonf/m^2) and friction angle ϕ of 40 deg are used in Eq. (36). Fig. 10 shows spatial distribution of the expected minimum local safety factors in both horizontal and transverse cross-sections for the case of the canyon slope equal to 1/2. In the region of 10 m and 20 m deep from the surface, local safety factor in the horizontal cross-section $(F_s|_{xy})_{\min}$ is smaller than that in the transverse cross-section $(F_s|_{xz})_{\min}$, especially in the region near the crest. And as the depth from the surface increases, the difference of the local safety factor between both cross-sections decreases, and at a depth of 40 m from the surface $(F_s|_{xy})_{\min}$ exceeds $(F_s|_{xz})_{\min}$.

Fig. 11 shows spatial distribution of the expected minimum local safety factors for the case of the canyon slope equal to 1/1. In this case even at a depth of 40 m from the surface, $(F_s|_{xy})_{\min}$ is smaller than $(F_s|_{xz})_{\min}$. These results indicate that when the earth dam is constructed in a narrow canyon and bounded by sloping walls, the local safety factor in the horizontal cross-section, which is not taken into account in the usual seismic analysis, can become an important item to estimate. Considering that in the static state shear stress is small in the horizontal cross-section and the gravity effect does not work during and after the earthquake, shear failure of the dam material in this cross-section may not lead to the collapse of the dam, although there still remains possibility that it is responsible for the material fracture which causes surface crack or land slide of the dam in the shallow region. Hence, evaluation of γ_{xy} and $(F_s)_{xy}$ in the horizontal cross section as well as those in the transverse cross-section should be required in the seismic analysis of earth dams especially when the dam is located in a narrow canyon and bounded sloping canyon walls.

8. CONCLUSIONS

A method of estimating the effect of spatial randomness of response characteristics on the seismic stability of earth dam was proposed. With this method spatial distribution of the expected maximum shear strain both in the horizontal and transverse cross-sections and also the distribution of the expected minimum local safety factor in the both cross-sections can be evaluated.

From the numerical estimation of the earth dam in the triangular canyon, it was made clear that the spatial randomness of the response characteristics of the earth dam has a considerable effect on shear strain in the horizontal cross-section during earthquake, especially in the case where the dam is constructed in a narrow canyon and surrounded by steep canyon walls. The proposed method, with its simplicity in the modeling and the calculation considering the randomness of both the response characteristics and the input earthquake motion, will be an effective tool for the preparatory estimation on the seismic stability of earth dams to be constructed in the narrow canyon and also in the assessment of seismic risk of the dam where the randomness associated with the response characteristics of the dam and the earthquake input motion are taken into account.

Acknowledgment: This work was partially supported by the National Center for Earthquake Engineering Research under NCEER Contract Number 873008 under NSF Master Contract Number ECE 8607591. The authors also acknowledge the support provided by the Central Research Institute of Electric Power Industry, Japan.

REFERENCES

1) Makdisi, F. I., Kagawa, T. and Seed, H. B. : Seismic Response of Earth Dams in Triangular Canyons, Journal of Geotechnical Engineering Division, ASCE, Vol. 109, No. GT 10, pp. 1328~1337, October, 1982.
2) Mejia, L. H. and Seed, H. B. : Comparison of 2-D and 3-D Analysis of Earth Dams, Journal of Geotechnical Engineering Division, ASCE, Vol. 109, No. GT 11, pp. 1383~1398, November, 1983.
3) Mejia, L. H., Seed, H. B. and Lysmer, J. : Dynamic Analysis of Earth Dams in Three Dimensions, Journal of Geotechnical Engineering Division, ASCE, Vol. 108, No. GT 12, pp. 1586~1604, December, 1982.
4) Harada, T. and Shinozuka, M. : Ground Deformation Spectra, Proc. of the 3 rd U. S. National Conference on Earthquake Engineering, pp. 2191~2202, 1986.
5) Harada, T. and Shinozuka, M. : Stochastic Analysis of Ground Response Variability for Seismic Design of Buried Lifeline Structures, Proc. of the 7 th Japan Earthquake Engineering Symposium, pp. 595~600, 1986.
6) Okamoto, S. : Introduction to Earthquake Engineering, Ohm Press (in Japanese), Tokyo, pp. 392~394, 1984.
7) Cartwright, D. E. and Longuet-Higgins, M. S. : The Statistical Distribution of the Maxima of a Random Function, Proc. of the Royal Society of London, Series A, Vol. 237, pp. 212~232, 1956.
8) Davenport, A. G. : Note on the Distribution of the Largest Value of a Random Function with Application to Gust Loading, Proc. of the Institution of Civil Engineers, Vol. 28, pp. 187~196, 1964.
9) Clough, R. Y. and Penzien, J. : Dynamics of Structures, McGraw-Hill Kougakusha, pp. 613~615, 1975.
10) Kanai, K. : Semi-empirical Formula for the Seismic Characteristics of the Ground, Bull. Earthquake Res. Inst., Univ. of Tokyo, Vol. 35, pp. 309~325, 1957.
11) Tajimi, H. : A Statistical Method of Determining the Maximum Response of a Building during an Earthquake, Proc. 2 nd World Conference on Earthquake Engineering, Tokyo and Kyoto, Vol. 11, pp. 781~798, July, 1964.
12) Ellingweed, B. R. and Batts, M. E. : Characterization of Earthquake Forces for Probability-based Design of Nuclear

Structures, Nuclear Regulatory Commission Report NUREG/CR-2945, 1982.
13) Dynamic Analysis and Earthquake-Resistant Design, Vol. 3, Energy Facilities (in Japanese), pp. 52~53, Gihodo Press, 1989.

(Received August 7 1989)